Colorimetric Sensing of Chlorpyrifos Pesticides Using Green Synthesized Silver Nanoparticles from Neem Root Extracts

Abidemi Mercy Babatimehin,[a,b,*] Oyebola Elizabeth Ogunbamowo,[a,c] Gabriel Olukayode Ajayi,[d] Ali El Gamal,[e] Talha Bin Emran,[f,g] Edwin Andrew Ofudje, [a] and Mohamed Hefnawy [h]

This study explores the colorimetric sensing of chlorpyrifos (CP) pesticides using neem root extracts-synthesized silver nanoparticles (NRE-AgNPs). The NRE-AgNPs were synthesized *via* a cost-effective bio-reduction method from neem (*Azadirachta indica*) and evaluated for their pesticide's colorimetric sensing property. Phytochemical analysis confirmed the presence of tannins (80.4 mg/mL), phenols (60.8 mg/mL), flavonoids (54.6 mg/mL), alkaloids (28.9 mg/mL), reducing sugars (59.1 mg/mL), and cardiac glycosides (47.6 mg/mL), which facilitated nanoparticle formation and stability. Scanning electron microscopy revealed nanoparticles with an average particle size of 68.3 nm, while energy-dispersive X-ray spectrum confirmed the presence of silver (0.14% atomic, 0.25% weight) alongside stabilizing organic compounds. UV-Vis spectroscopy confirmed NRE-AgNP synthesis with a surface plasmon resonance peak at 405 nm. The nanoparticles responded sensitively to the presence of the chlorpyrifos, especially at 300 to 350 nm, marking a clear deviation from their original 405 nm signature, thus confirming the viability of AgNPs as an optical sensor. This study underscores the potential of neem root-based AgNPs as a sustainable and eco-friendly solution for pesticide sensing, offering promising applications in the environmental field.

DOI: 10.15376/biores.20.3.6948-6965

Keywords: Azadirachta indica; Colorimetric sensing; Nanoparticles; Pesticides; Phytochemicals

Contact information: a: Department of Chemical Science, Mountain Top University, Lagos- Ibadan Expressway, Move, Ogun State, Nigeria; b: Department of Biochemistry, Lagos State University, Ojo, Lagos, Nigeria; c: Department of Medical Biochemistry, Lagos State University College of Medicine, Ikeja, Lagos, Nigeria; d: Department of Biochemistry, Mountain Top University, Lagos - Ibadan Expressway, Move, Ogun state, Nigeria; e: Department of Pharmacognosy, College of Pharmacy, King Saud University, Riyadh 11451, Saudi Arabia; f: Department of Pathology and Laboratory Medicine, Warren Alpert Medical School, Brown University, Providence, RI 02912, USA; g: Department of Pharmacy, Faculty of Health and Life Science, Daffodil International University, Dhaka 1207, Bangladesh; h: Department of Pharmaceutical Chemistry, College of Pharmacy, King Saud University, Riyadh 11451, Saudi Arabia;
**Corresponding author: abidemibabatimehin530@gmail.com*

INTRODUCTION

The extensive use of pesticides has led to severe environmental contamination, particularly in soil and water systems, posing risks to aquatic life and human health. Further, a 2020 study published in World Development highlights that income convergence across countries could lead to a significant rise in world food demand by 2050 (Fukase and Martin 2020). After pesticides are used to treat pests, residues are left

in agricultural soil that harm terrestrial and aquatic ecosystems (Karami-Mohajeri and Abdollahi 2011). Organophosphate (OP) pesticides were introduced in the 1950s for pest control and have since become the most widely used insecticides in agriculture. Their popularity stems from their high toxicity to pests and lower persistence in soil compared to chlorinated pesticides such as methoxychlor (Foong *et al*. 2020). Although OPs are less harmful to non-targeted animals, such as birds and fish, their use has significantly grown in recent decades, contaminating the food web (Intisar *et al*. 2022), as residues of OPs have been found in several environments, including agricultural crops and water sources (Bose *et al.* 2021). Chlorpyrifos (CP) is a toxic OP pesticide (class II) that is widely used in agriculture, horticulture, forestry, and household use, as well as public health and pest management (Foong *et al*. 2020). Multiple studies have linked CP to reduced sperm activity and adverse effects on the liver and kidneys (Zhang *et al*. 2021; Zhang *et al*. 2023). Prenatal exposure has been linked to small head size, delayed brain development, low birth weight, and neurological disorders in offspring (Berna *et al.* 2024).

Electrochemical sensors offer many advantages but face key challenges that limit their broader application. Achieving high selectivity in complex sample matrices is difficult due to potential interference from other substances. Sensor fouling from biological or chemical buildup can degrade performance, while environmental factors such as temperature and pH affect stability and reproducibility (Jaya *et al*. 2022). These sensors often require frequent calibration due to signal drift, and their integration into portable systems can be technically demanding (Jaya *et al*. 2022). Mass-based sensors such as Quartz Crystal Microbalance (QCM) and Surface Acoustic Wave (SAW) though highly sensitive, label-free sensors are valuable in chemical detection but are affected by environmental factors including temperature and humidity (Ali 1999). They also typically require the immobilization of selective receptor molecules, and their fragility and sensitivity to external conditions limit their suitability for field applications. Spectroscopy such as Nuclear Magnetic Resonance (NMR), Mass Spectrometry (MS), and Raman Spectroscopy are widely employed in pesticide analysis due to their high-resolution capabilities, particularly for identifying complex or unknown mixtures (Abu *et al*. 2024). Despite their analytical power, these methods are generally costly, energy-intensive, and require significant sample preparation and laboratory infrastructure, making them impractical for real-time field applications (Abu *et al*. 2024). To address these limitations, optical sensors have emerged as a promising alternative, enabling the detection of pesticides at low concentrations even in complex matrices. This advancement supports more effective monitoring of pesticide levels to ensure safety in food and the environment at low cost.

Recently, nanotechnology has emerged as a valuable pesticide sensing and treatment technique. Nanomaterials refer to materials with nanoscale surface structure or dimensions. Nanomaterials are created using traditional (chemical and physical) and green processes. They offer advantages such as producing nanoparticles (NPs) with specific shapes and sizes, scalability, and numerous applications, including electrical, energy conservation, catalytic activity, and disease therapy (Agarwal *et al*. 2019; Ying *et al*. 2022). Green synthesis, known as biosynthesis, is a cost-effective, safe, and ecologically friendly process that uses microorganisms (such as bacteria, actinomycetes, yeast, fungus, and algae) and plant extracts to decrease and stabilize metal or metal oxide precursors, resulting in NPs (Jeevanandam *et al*. 2022; Ying *et al*. 2022). Active

metabolites or phytochemicals from microorganisms or plant extracts are used for reduction and capping stages (Villagrán *et al*. 2024).

Nanoparticles have potential to be used as tools for the detection and identification of metal ions, leveraging their unique optical and chemical properties. The primary mechanisms involved in metal ion sensing using NPs include surface plasmon resonance (SPR), NP aggregation leading to observable color changes, complex formation, and redox reactions (Du *et al*. 2012).

The present work involved the preparation and usage of silver nanoparticles (AgNPs) in a system for detection of pesticides. The choice of neem tree root extract for the synthesis of AgNPs, rather than using chemical methods, is primarily due to its eco-friendly nature. Neem extract serves as a green reducing agent, eliminating the need for toxic chemicals such as sodium borohydride or hydrazine, which pose significant environmental hazards (Roy *et al*. 2017; Babatimehin *et al*. 2025). This approach aligns with green chemistry principles, reducing chemical waste, and minimizing pollution. Another major advantage is the biocompatibility of neem-based AgNPs, as chemically synthesized NPs often carry risks of toxicity, whereas biogenic AgNPs are generally safer for biomedical and pharmaceutical applications (Chaudhary *et al*. 2017). This makes them more suitable for drug delivery, and wound healing treatments.

Neem extract also plays a dual role in AgNPs synthesis by acting as both a reducing and stabilizing agents. The presence of bioactive compounds such as flavonoids, tannins, terpenoids, and alkaloids helps reduce Ag^{+} ions to AgNPs while simultaneously stabilizing the formed NPs. This eliminates the need for additional stabilizing agents, simplifying the synthesis process. In this study, AgNPs were synthesized *via* a cheap bio-reduction method from root extracts of *Azadirachta indica.* The study explored the multifaceted properties of green synthesized NPs, focusing on their optical characteristics for pesticides detection. The study explores the optical properties of AgNPs particularly their surface plasmon resonance (SPR) in colorimetric sensor of CP using neem root-synthesized AgNPs, assessing their efficiency under varying environmental conditions.

MATERIALS AND METHODS

Reagents

The high-purity reagents used were purchased from Sigma Aldrich in Cape Town, South Africa. All glassware was cleaned with distilled water and dried in an oven.

Collection of Sample

The roots of *Azadirachta indica* (Neem) were harvested from mature trees within the Lagos State University Zoological Garden, Nigeria. Botanical authentication was conducted by experts from the Department of Botany at Lagos State University, and a voucher specimen was deposited in the department's herbarium. The collected roots were thoroughly washed multiple times with distilled water to remove any impurities and then air-dried at room temperature for 10 days.

Preparation of Neem Root Extract (NRE) Sample

The dried roots of *Azadirachta indica* were chopped into smaller pieces and ground into a fine powder. A 5 g sample of the powdered roots was soaked in 100 mL of distilled water and stirred continuously on a magnetic stirrer for 24 hours. The mixture was then filtered using Whatman No. 1 filter paper, and the resulting extract was stored in a refrigerator for use in NPs synthesis.

Phytochemical and Qualitative Analysis of the NRE-AgNPs

This procedure followed the methods described by Mudhafar *et al*. (2020) and Babatimehin *et al*. (2025). The NRE plant extract was analyzed using GC-MS to identify its phytochemical constituents. The analysis was performed using a 7820A gas chromatograph paired with a 5975C inert mass spectrometer, featuring a triple-axis detector, and an electron impact source (Agilent Technologies). Potential compounds were scanned at a rate of 2.62 s/scan from *m/z* 30 to 550 amu and identified by comparing the obtained mass spectral data with the NIST 14 Mass Spectral Library.

Fig. 1. Neem Root (*Azadirachta indica*)

Optimization Study in the Synthesis of Silver Nanoparticle

This analysis was carried out following the methods of Mudhafar *et al.* (2020) and Babatimehin *et al*. (2025). A 100 mL solution of 1 mM silver nitrate was mixed with 10 mL of plant root extract stock solutions at varying concentrations (0.2 to 50 mg/L). The mixtures were incubated at different temperatures ranging from 25 to 100 °C while being agitated on a shaker at 120 rpm. After 1 h of shaking, absorbance was measured using a UV-Vis spectrophotometer (SM 7504, Shanghai, China) over a wavelength range of 300 to 600 nm. The experiment was repeated under different conditions, varying pH levels, temperatures, and plant extract concentrations. The synthesis of AgNPs, is usually affected by these factors which can cause reduction or acceleration of the rate process and nanoparticle properties. In our experiments, the synthesis was conducted under ambient temperature using a 60 W incandescent lamp.

Characterization of Biosynthesized NRE-AgNPs

The powder samples were prepared by first centrifuging the colloidal silver nanoparticle solution to collect the nanoparticles. The pellet was then washed with distilled water. After washing, the samples were dried at 105 °C in a hot air oven for 4 h until a consistent dry powder was obtained. A UV-Visible spectrophotometer (SM 7504, Shanghai, China) was used to characterize and detect the synthesized NRE-AgNPs. Fourier transform infrared spectroscopic (FT-IR) analysis was performed on both the NRE and the synthesized NRE-AgNPs using a model CARY630 NBY (Thermo Fisher Scientific Instrument). The KBr pellet method was utilized, where a 1:99% mixture of NRE-AgNPs powder and KBr was finely ground using a mortar and pestle, then compressed into a 2 mm diameter pellet. FT-IR spectra were recorded within the 400 to 4000 cm^{-1} range, with a resolution of 4 cm^{-1} and 64 scans. X-ray diffraction (XRD) analysis was performed to assess the crystalline structure of the NRE-AgNPs, scanning across a 2θ range of 10° to 70°. Diffraction peaks were indexed according to the Joint Committee on Powder Diffraction Standards (JCPDS).

Scanning electron microscopy coupled with energy-dispersive X-ray spectroscopy (SEM-EDS) was employed to examine the surface morphology and elemental composition of the NRE-AgNPs. Imaging was conducted using a Hitachi S-3000H SEM (Japan) operating at 15 kV, while elemental composition was determined using the integrated EDX system. The particle size distribution of the NRE-AgNPs was measured with a Nanotrac system, utilizing Microtrap FLEX 10.5.2 software for data processing. Prior to analysis, 0.1 g of the sample was dispersed in 50 mL of Millipore water within a 100 mL beaker and sonicated for 10 min to minimize particle agglomeration.

Chlorpyrifos Pesticides Detection

The synthesized silver nanoparticle was used to sense pesticides by the method described by Kushwaha *et al*. (2020). Equal volumes of prepared nanoparticles and CP were combined at room temperature, and the colorimetric responses and absorption intensity changes were checked using UV-vis Spectroscopy wavelength of 300 to 500 nm. The readings were taken in duplicate, and the average value was recorded.

RESULTS AND DISCUSSION

Table 1. Qualitative and Quantitative Analysis of Neem Root Extract (mg/mL)

	Tannin	Phenol	Saponin	Alkaloid	Reducing sugar	Cardiac glycoside	Flavonoid
(mg/mL)	80.38	60.75	17.70	28.90	59.11	47.64	54.56

The qualitative and quantitative analysis of NRE (Table 1) revealed significant concentrations of bioactive compounds, each contributing to its medicinal properties and its effectiveness in AgNPs synthesis. Tannins, present in the highest concentration (80.4 mg/mL), act as strong reducing agents that facilitate the conversion of Ag^{+} ions into elemental silver (Ag^{0}), enhancing nanoparticle formation, Phenols (60.8 mg/mL), the second most abundant compound, play a dual role as reducing and capping agents, promoting AgNP synthesis while preventing aggregation (Roy *et al.* 2017; Chhangte *et al.* 2021). Flavonoids (54.6 mg/mL) are also efficient metal ion reducers and stabilizing

agents, ensuring nanoparticle stability while contributing anti-inflammatory benefits (Roy *et al.* 2017; Chhangte *et al.* 2021). Reducing sugars (59.1 mg/mL) aid in AgNP formation by donating electrons for Ag^+ ion reduction, while cardiac glycosides (47.6 mg/mL) contribute to nanoparticle stability and offer cardioprotective and anticancer effects. Alkaloids (28.9 mg/mL) function as capping and stabilizing agents, preventing nanoparticle aggregation while enhancing their analgesic properties (Roy *et al.* 2017; Chhangte *et al.* 2021). Saponins, present in the lowest concentration (17.7 mg/mL), may play a minimal role in nanoparticle formation but contribute to solubilization and dispersion, improving bioavailability. This further supports NRE as an eco-friendly and sustainable alternative for nanoparticle synthesis (Matam *et al*. 2021; Ritu *et al*. 2023).

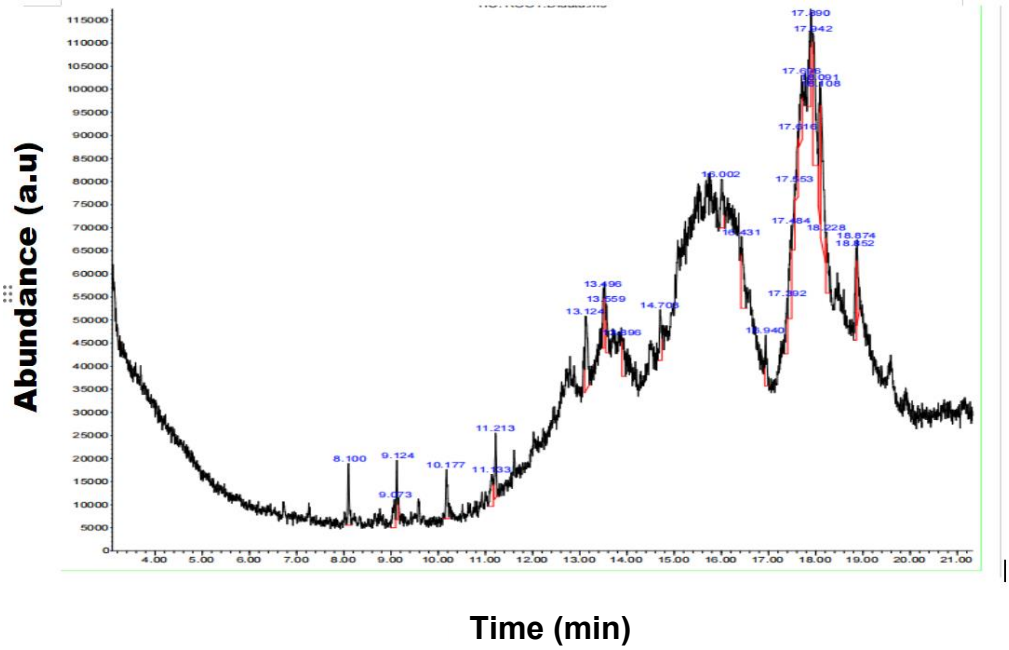

Fig. 2. GC-MS of neem root extract

The phytochemicals identified in the GC-MS analysis of NRE, as displayed in Fig. 2, play crucial roles in the synthesis of AgNPs by acting as reducing, stabilizing, and capping agents. Some of the compounds present in the NRE that are likely involved in reducing Ag^+ to Ag^0, initiating the nanoparticle formation are methoxyacetic acid, 3-tridecyl ester, methoxyacetic acid, 3-pentadecyl ester, 9-hexadecenoic acid methyl ester, carbonic acid, 2-ethylbutyric acid, 2-hexyl ester, tetracontane, oxalic acid, and cyclobutyl heptadecyl ester. These carboxylic acid derivatives and esters provide hydrogen atoms or electrons, reducing Ag^+ ions into elemental Ag^0 nanoparticles (Uznanski *et al*. 2017). Those compounds identified by the GC-MS that can act as capping agents to prevent aggregation and stabilize nanoparticles are hentriacontane, heneicosane, nonyl tetracosyl ether, eicosyl nonyl ether, dodecanoic acid, 2-tert-butyl-5,5-dimethyl-3-oxo-1-pyrroline, diazoprogesterone, tricyclo[5.4.3.0(1,7)]tetradecane-3,6-diol, phthalic acid, and benzothiazole. These compounds contain long-chain hydrocarbons, ethers, or carbonyl functional groups, which bind to the nanoparticle surface, preventing aggregation and stabilizing their structure (Javed, *et al*. 2020; Sidhu *et al*. 2020). Some compounds were also present in the extract as provided by the GC-MS analysis. Some of these could enhance the antioxidant, or catalytic properties of NRE-AgNPs, and they include the likes

of 2,5-dimethyl-5-ethyl-2-oxazoline, pentadecanoic acid, 2,4-hexadienoanilide, 1,5,9,13-tetradecatetraene, 3-nonyne, and octahydro-trans2(1H)-pyridinone. These compounds, containing amide, alkyne, and conjugated unsaturated systems, may contribute to the enhanced catalytic activity of NRE-AgNPs. Such compounds as isobutyl nonyl carbonate, -octanol, 2-butyl-heptane may likely act as solubilizing agents, enhancing extraction efficiency, while decyl ester may enhance hydrophobic interactions, improving nanoparticle stability. Thus, the NRE contains a mix of reducing, stabilizing, and bioactive compounds, making it an efficient and eco-friendly agent for AgNP synthesis (Tshilumbu *et al.* 2014).

The FT-IR spectra of the NRE and AgNPS provided valuable insights into its chemical composition, revealing the presence of various bioactive compounds responsible for its medicinal properties and its role in AgNPs synthesis, as shown in Fig. 3. The broad peak observed around 3458 cm^{-1} corresponds to either O-H or -NH stretching vibrations, which are typically associated with hydroxyl groups in phenols, flavonoids, tannins, amine, and alcohols (Taha *et al*. 2020; Babatimehin *et al*. 2025). This indicates strong hydrogen bonding interactions, commonly found in polyphenolic compounds, which play a crucial role in antioxidant activities. Peaks at 2922.2 cm^{-1} and 2855.1 cm^{-1} correspond to C-H stretching vibrations of alkanes, which suggest the presence of long-chain hydrocarbons, fatty acids, and terpenoids. These compounds are important for nanoparticle stabilization, as they help form a hydrophobic layer around AgNPs, preventing aggregation and ensuring their stability (Taha *et al*. 2020; Babatimehin *et al*. 2025). A strong peak at 1714.4 cm^{-1} is attributed to C=O stretching vibrations of carbonyl functional groups found in carboxylic acids, esters, ketones, or aldehydes and the presence of this peak suggests that compounds such as flavonoids, tannins, and organic acids are present, which act as reducing agents during the conversion of Ag^{+} ions into Ag^{0} nanoparticles (Mercija and Nevaditha 2022; Javid *et al*. 2023).

Similarly, the peak at 1638.3 cm^{-1} is associated with C=C stretching vibrations from aromatic rings or amide groups, further indicating the presence of phenolic compounds, flavonoids, and alkaloids, which contribute to antioxidant property (Mercija and Nevaditha, 2022; Javid *et al*. 2023). The peak at 1457.4 cm^{-1} corresponds to C-H bending vibrations, which are commonly observed in lipids and fatty acids. This suggests the presence of compounds that may enhance hydrophobic interactions, aiding in the stability of bioactive molecules. Another peak at 1375.4 cm^{-1} is associated with C-O stretching vibrations, indicative of carboxyl (-COOH) or phenol (-OH) groups and these functional groups are essential in reducing and stabilizing nanoparticles during green synthesis processes (Taha *et al*. 2020; Javid *et al*. 2023).

The peak at 1151.7 cm^{-1} corresponds to C-N stretching vibrations, characteristic of alkaloids, amines, or proteins. Additionally, peaks at 1028.7 and 872.2 cm^{-1} indicate C-O and C-H deformation vibrations, suggesting the presence of polysaccharides, phenolic rings, or flavonoids, which further contribute to nanoparticle capping and bioactivity (Taha *et al*. 2020; Javid *et al*. 2023). The FT-IR spectrum confirms the presence of key functional groups, such as O-H, C=O, C=C, and C-O, indicating a rich composition of phenols, flavonoids, tannins, and organic acids. These compounds serve as reducing agents that facilitate the conversion of Ag^{+} to Ag^{0}, initiating AgNP formation, thus corroborating the results from GC-MS analysis. The C-H and C-O vibrations further indicate the presence of long-chain hydrocarbons, fatty acids, and terpenoids, which act as stabilizing agents to prevent nanoparticle aggregation. Additionally, the presence of C-N and amide groups suggests that alkaloids and proteins enhance the bioactivity of

synthesized nanoparticles. In the NRE spectrum, a strong broad band is seen around 3400 cm^{-1}, which corresponds to O-H and N-H stretchings was observed. However, this peak shifted to around 3395 cm^{-1}, suggesting interaction with AgNPs. A peak which corresponds to carbonyl (C=O) stretching was seen, but this peak shifted to around 1695 cm^{-1} and there was also a reduction in the peak intensity in NRE-AgNPs, indicating possible binding of AgNPs with carbonyl groups. The shifts in peaks, intensity reduction, and disappearance of other peaks in NRE-AgNPs suggest that functional groups from the neem root extract (*e.g.*, hydroxyl, carbonyl, and amine groups) play a role in reducing and stabilizing AgNPs. This confirms the biomolecule-mediated synthesis of NRE-AgNPs, where phytochemicals act as reducing and capping agents.

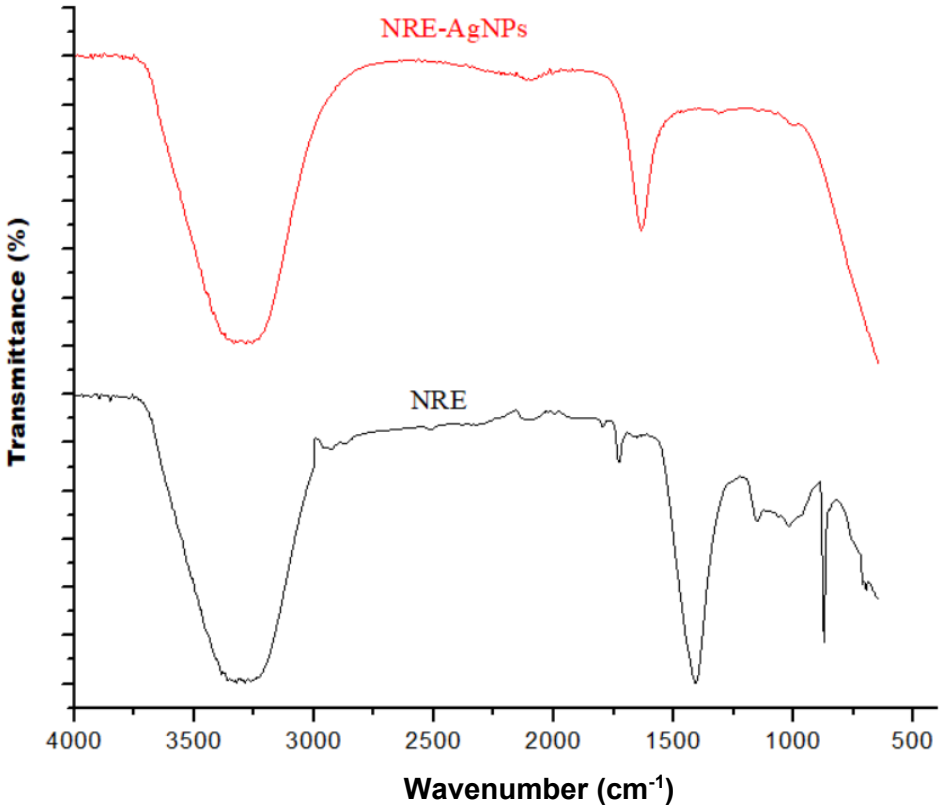

Fig. 3. FT-IR spectral of neem root extract

The SEM images of the neem root as well as that of the NRE-AgNPs formed are displaced in Fig. 4. The image of the neem root (Fig. 4a) displays a rough, porous structure with irregularly shaped particles. There are multiple small, granular formations suggesting the presence of cell debris or soil particles adhered to the root surface. The neem root's surface is likely covered with fibrous material, possibly remnants of root hairs. The presence of inorganic materials (silica or mineral deposits) on the root surface is also possible. The SEM image of the green synthesized NRE-AgNPs (Fig. 4b) shows nanoparticle aggregation with some irregular shaped clusters, suggesting that the silver nanoparticles (AgNPs) had aggregated into larger formations. These large, porous structures could indicate the presence of biogenic capping agents, which are common in green synthesis methods using plant extracts. The morphology of some of the NPs have spherical or semi-spherical shapes, which are typical in green synthesis methods. Furthermore, the high porosity and small protrusions suggest the involvement of organic

molecules that aid in nanoparticle stabilization. Figure 4c confirmed the formation of nanomaterials in the range of 10 to 1000 nm with average particle size distributions of 48.3 nm.

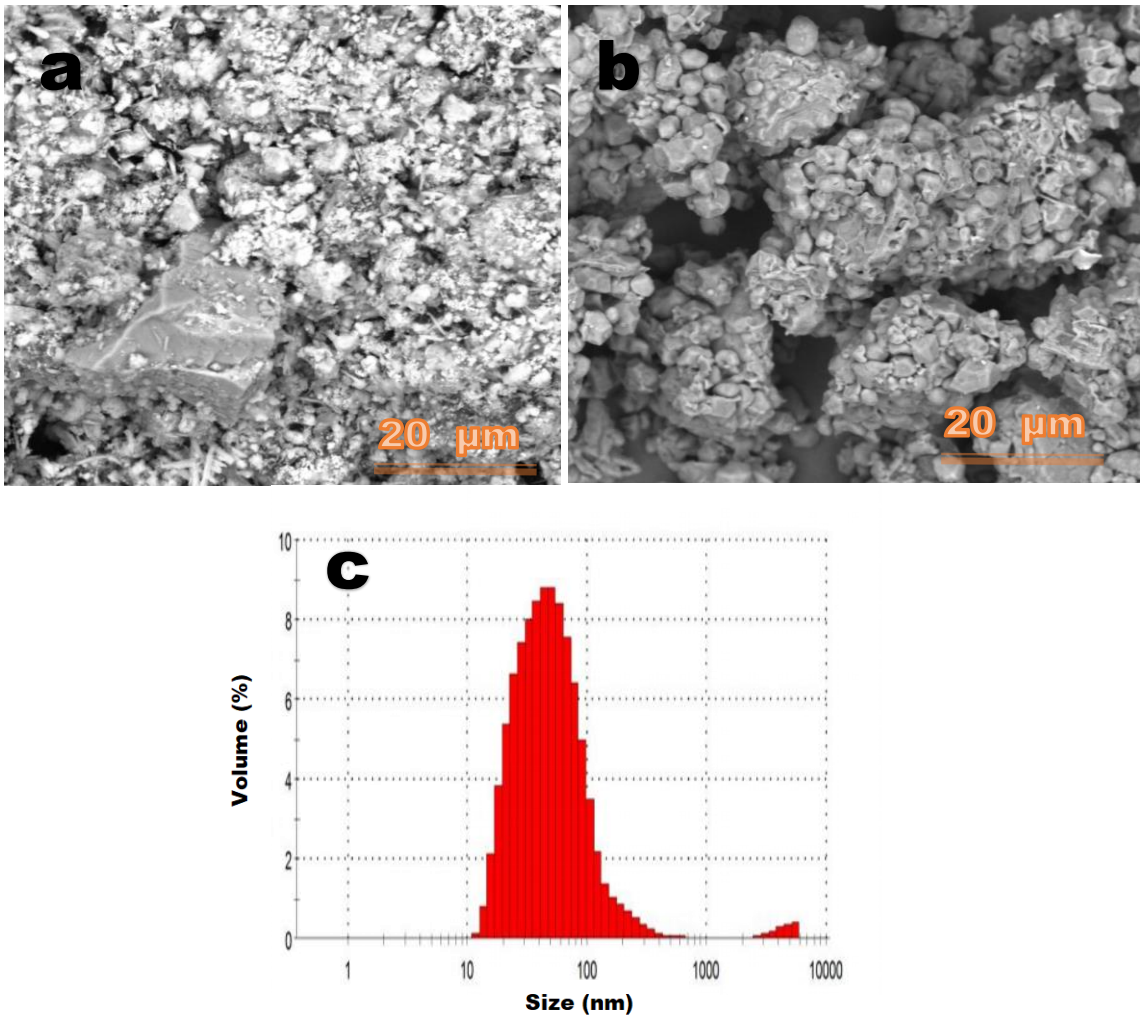

Fig. 4. SEM images of (a) neem root, (b) synthesized NRE-AgNPs, and (c) particle size distributions of synthesized NRE-AgNPs

The XRD pattern of NRE-AgNPs confirms their crystalline nature, as indicated by the presence of sharp and intense diffraction peaks. The most prominent peak around 38.13° (2θ) corresponds to the (111) reflection of face-centered cubic (FCC) silver, while additional peaks near 44.03°, 64.12°, and 77.02° can be attributed to the (200), (220), and (311) reflections, respectively (Hassanien *et al*. 2018; Patil and Chougale 2021). These peaks align well with the standard JCPDS card number 04-0783, confirming the formation of metallic AgNPs without significant oxidation.

The crystallite size was estimated using the Debye-Scherre equation below (Hassanien *et al*. 2018):

$$D = 0.94 / \beta \cos\theta \quad (1)$$

where, D represents the crystallite size (nm), λ is the wavelength of the radiation (0.15418 nm), β is the full width at half maximum (FWHM) in radians, and θ is half of the Bragg angle. Using the plane for the (111), the average crystallite size of NRE-AgNPs was determined to be 44.2 nm which is closely matched the particle size obtained earlier. The absence of impurity peaks further indicates effective stabilization by phytochemicals present in the extract. The XRD results confirm that the synthesized NRE-AgNPs possess a high degree of crystallinity, similar to those obtained through chemical synthesis.

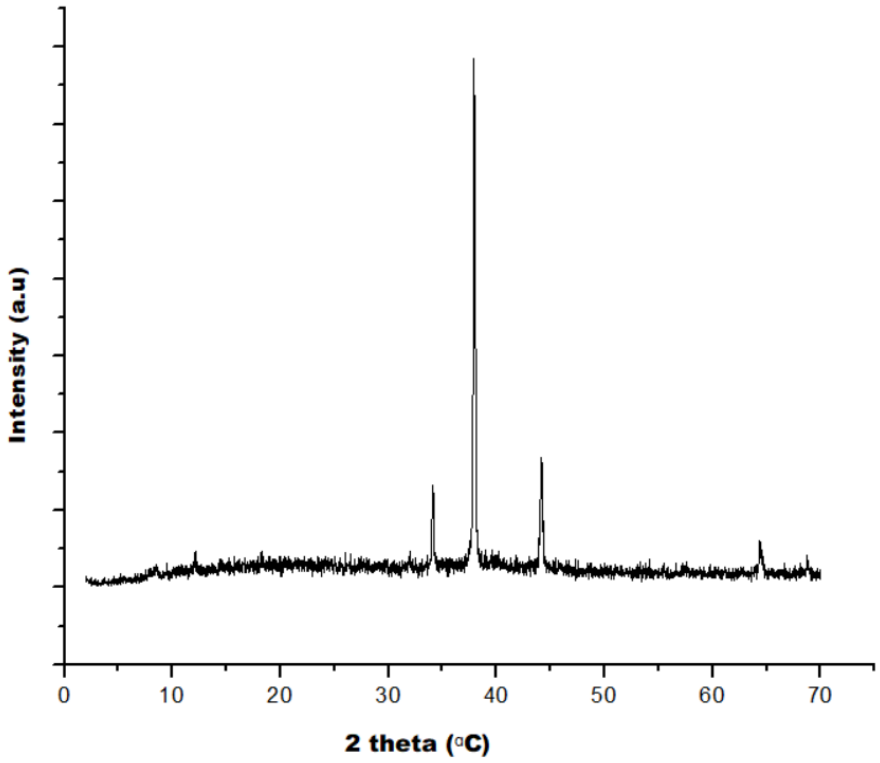

Fig. 5. XRD spectrum of NRE-AgNPs

The elemental analysis of AgNPs synthesized using NRE (Fig. 6) reveals a composition dominated by oxygen (31.34% atomic, 28.06% weight) and carbon (35.14% atomic, 22.78% weight), suggesting that the NPs were heavily coated with organic biomolecules from the neem extract. The presence of nitrogen (4.72% atomic, 3.57% weight) and sulfur (2.35% atomic, 1.04% weight) further supports the idea that proteins or amino acids may act as stabilizing agents. Additionally, significant amounts of silicon (16.1% atomic, 24.4% weight), aluminum (7.0% atomic, 10.2% weight), and iron (3.2% atomic, 9.8% weight) indicate possible natural components of the extract. Despite being the target material, silver is present at a relatively low concentration (0.14% atomic, 0.25% weight), suggesting that the NPs are embedded in or capped with a substantial amount of non-metallic material.

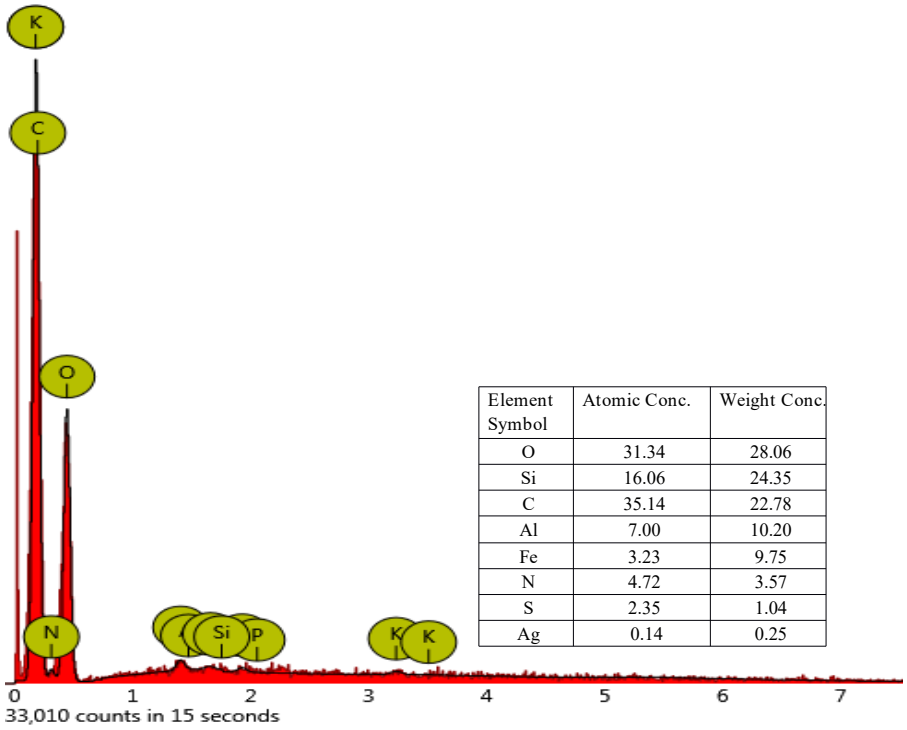

Element Symbol	Atomic Conc.	Weight Conc.
O	31.34	28.06
Si	16.06	24.35
C	35.14	22.78
Al	7.00	10.20
Fe	3.23	9.75
N	4.72	3.57
S	2.35	1.04
Ag	0.14	0.25

Fig. 6. EDS of NRE-AgNPs from the neem extract

Optimization Studies on the Synthesis of NRE-AgNPs

Effects of neem concentration and reaction time

The synthesis of NRE-AgNPs was visually confirmed through color changes. Upon adding silver nitrate ($AgNO_3$) to the NRE, the solution transitioned from light yellow to deep brown (Fig. 7a). This color change indicates the formation of NRE-AgNPs, as the reducing agents in the NRE facilitate the reduction of silver salts to silver metal. Natural compounds such as alkaloids, terpenoids, and flavanones in the extract contribute to this reduction process. Figure 7b presents the UV-Vis spectra of AgNPs synthesized using *Azadirachta indica* root extract at different reaction times and concentrations. As the reaction time increased from 60 to 120 min, the absorption peak intensity also increased. The optimal incubation time for AgNPs synthesis was determined to be 75 min, beyond which no further rise in absorbance was observed. The spectra revealed a strong surface plasmon resonance (SPR) peak at approximately 400 nm, consistent with AgNP formation. A study by Ismail *et al*. (2019) reported that chemically synthesized AgNPs using gallic acid exhibited a narrow SPR band with an absorbance maximum at 396 nm, confirming the formation of AgNPs. Mahmood *et al*. (2021) investigated the SPR properties of AgNPs colloids prepared *via* an electrochemical method. Their findings indicated that the wavelength of the maximum absorption band for AgNPs ranged from approximately 350 nm to 550 nm, depending on particle size and synthesis conditions. After 75 min, the reaction mixture's color stabilized, indicating the complete consumption of silver ions (Babatimehin *et al.* 2025). At lower NRE concentrations (<12.5 mg/mL), a faint absorbance band was observed. However, increasing the concentration to 50 mg/mL resulted in a significant rise in peak intensity. The absorbance strength consistently increased with higher extract concentrations (Fig. 7b). Additionally, a bathochromic shift (red shift) was noted, with

the absorbance peak shifting slightly from 400 nm to 415 nm, indicating a shift toward longer wavelengths as the extract concentration increased.

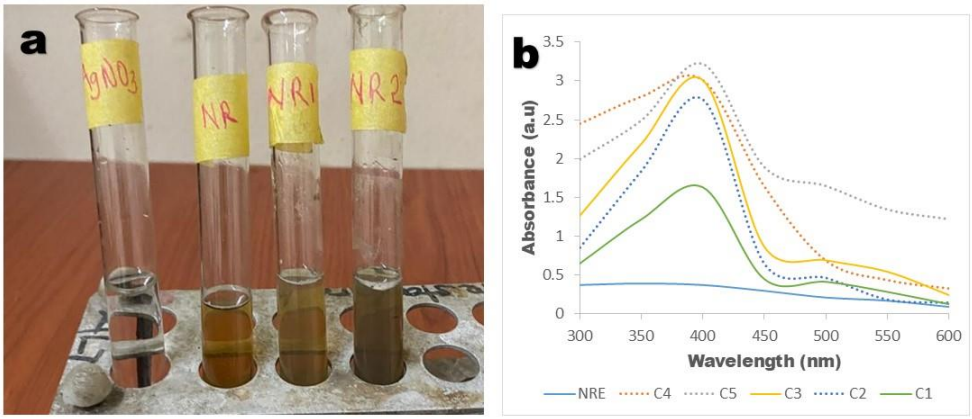

Fig. 7. (a) Color of solutions: $AgNO_3$, NRE, NR1: NRE with $AgNO_3$ for 1 h, NR2: NRE with $AgNO_3$ after 6 h, and (b) UV–Vis spectra of synthesized NRE-AgNPs at 6 h at different NRE concentrations of *C1 = 100, C2 = 50, C3= 25, C4 = 12.5, C5 = 6.25.*)

Effect of pH and Temperature

The pH of the reaction medium significantly influenced the formation and stability of biogenic AgNPs by altering the electrical charges of biomolecules and affecting capping efficiency. As shown in Fig. 8a, increasing the pH led to a rise in absorbance, indicating reduced nanoparticle size and polydispersity, with the most notable change occurring between pH 2.0 and 8.0. The absorption maxima shifted from 340 to 450 nm between pH 6.0 and 8.0, suggesting pH 8.0 as optimal for NRE-AgNP synthesis. Similar observations were made by Khalil *et al*. (2014), who reported that AgNPs synthesized from olive leaf extract were smaller and more uniform at basic pH 8 compared to acidic pH 3, due to enhanced antioxidant activity. Their TEM analysis confirmed size reduction at higher pH, along with a blue shift in absorption peaks. Verma and Mehata (2015) also found that pH affects AgNP synthesis using neem extract, noting a shift in absorption maxima from 383 to 415 nm as pH increased from 9 to 13. However, excessive alkalinity led to particle aggregation and a red shift in the SPR band due to instability.

Temperature also played a critical role in the AgNP synthesis. As shown in Fig. 8b, increasing temperature (25 to 100 °C) accelerated silver salt reduction and caused a blue shift in the absorption peak from 400 to 350 nm, indicating smaller particle formation at higher temperatures. Lee *et al.* (2014) demonstrated temperature-dependent optical shifts in AgNPs synthesized under green LED irradiation, with SPR peak variations due to changes in size and shape. Muthuswamy *et al*. (2010) observed that elevated temperatures (20 to 60 °C) increased AgNP productivity and zeta potential in *Curcuma longa*-based synthesis, though particle size also tended to increase. In contrast, Babatimehin *et al*. (2025) found a slight blue shift (400 to 395 nm) when increasing temperature from 25 to 35 °C using neem extract, further supporting temperature sensitivity in AgNP formation.

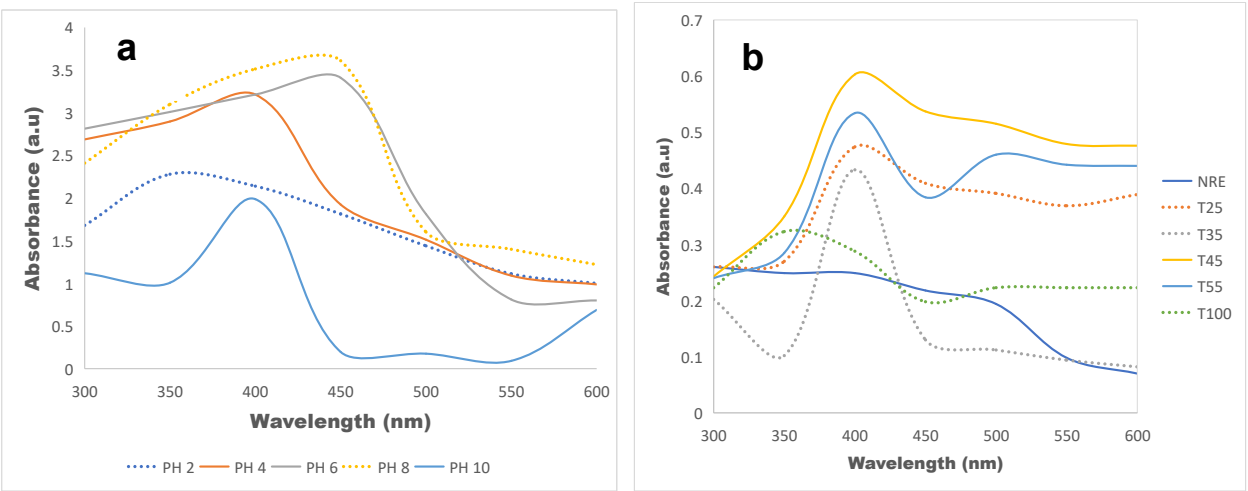

Fig. 8. Absorption spectra of synthesized NRE-AgNPs at (a) various pH (pH 2.0-10.0), and (b) various temperatures (25 to 100 ºC) where (N = neem root extract, *T25=25* ºC, *T35=35* ºC, *T45=45* ºC, *T55=50* ºC, *T100=100* ºC)

Sensing Tests with Chlorpyrifos by AgNPs

The graph in Fig. 9 illustrates the UV-Vis absorbance behavior of silver nanoparticles (AgNPs) resulting from exposure to different concentrations of chlorpyrifos across a wavelength range from 300 to 600 nm. From the graph, it is evident that the highest absorbance intensities occurred at 300 and 350 nm for all chlorpyrifos concentrations, particularly peaking at 750 ppm. As the wavelength increased beyond this region, the absorbance decreased consistently across all concentrations. This behavior signifies a blue shift in the SPR peak, indicating that the dominant absorbance had shifted from the original 400 nm toward shorter wavelengths (Kushwaha *et al*. 2020). A blue shift typically reflects a decrease in particle size, a reduction in nanoparticle aggregation, or changes in the surface electron density effects that can be triggered by molecular interactions with chlorpyrifos (Sarkar and Das 2018).

The blue shift observed here suggests that the presence of chlorpyrifos influenced the structural or surface chemistry of the AgNPs (Shikha *et al.* 2021). Rather than promoting aggregation (which would cause a red shift), chlorpyrifos appears to have induced disaggregation or particle stabilization, resulting in smaller effective nanoparticle sizes or a modified electronic environment around the particles (Shikha *et al.* 2021). This spectral behavior underscores the potential of AgNPs to function as a sensitive and efficient colorimetric sensor for chlorpyrifos. Notably, the response was most pronounced at 750 ppm, suggesting this may represent the optimal concentration for detection. At 1000 ppm, a slight decline in absorbance is observed, possibly due to nanoparticle saturation or instability at higher chlorpyrifos levels.

Sarkar and Das (2018) studied the interaction between chlorpyrifos and polyvinylpyrrolidone (PVP)-stabilized silver nanohexagons. Their findings revealed a blue shift in the surface plasmon resonance (SPR) peak following chlorpyrifos exposure, which they attributed to an etching effect on the silver nanocrystals. This etching reduced the nanoparticle size, resulting in the observed shift toward shorter wavelengths. Shikha *et al.* (2021) examined the interactions between borohydride-stabilized silver nanoparticles and several organophosphate pesticides, including chlorpyrifos. Their results showed that chlorpyrifos had limited interaction with the silver nanoparticles, leading to minimal aggregation. This absence of significant aggregation indicates that

chlorpyrifos may play a stabilizing role, inhibiting the red shift commonly associated with nanoparticle clustering.

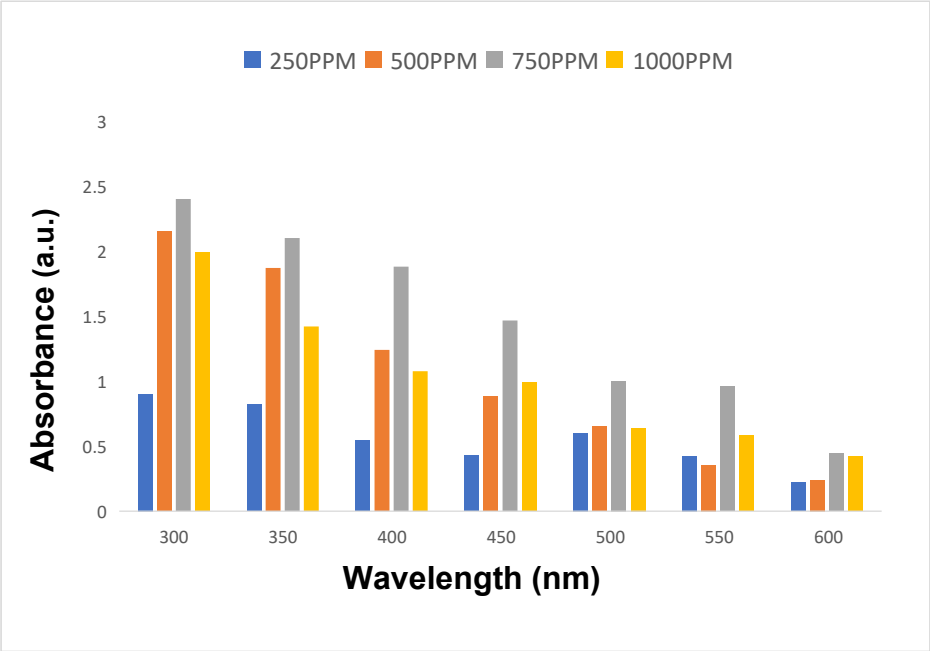

Fig. 9. UV–vis of optical response of AgNPs in sensing chlorpyrifos at varying concentrations.

CONCLUSIONS

This study explored the synthesized silver nanoparticles (NRE-AgNPs) derived from neem (*Azadirachta indica*) for the detection of chlorpyrifos pesticides. Key findings were as follows:

1. The green synthesis of NRE-AgNPs was achieved using neem root extract facilitating eco-friendly AgNP synthesis.
2. Fourier transform infrared (FT-IR), scanning electron microscope (SEM), energy dispersive spectroscopy (EDS), and X-ray diffraction (XRD) confirmed the synthesis of AgNPs.
3. A blue shift from 400 nm to lower wavelengths between 300 and 350 nm upon chlorpyrifos exposure highlights a direct and measurable interaction between the pesticide and AgNPs.
4. The silver nanoparticles can therefore be deployed as a viable tool for developing rapid, low-cost, and effective optical sensors for environmental monitoring and pesticide residue detection.

ACKNOWLEDGMENTS

The authors extend their appreciation to the financial support via the Ongoing Research Funding program, (ORF-2025-754), King Saud University, Riyadh, Saudi Arabia, for funding this research

REFERENCES CITED

Abu, B. N., Fronziy, M., and Shapter, J. G. (2024). "Surface-enhanced Raman spectroscopy using a silver nanostar substrate for neonicotinoid pesticides detection," *Sensors* 24(2), article 373. DOI: 10.3390/s24020373

Agarwal, H., Nakara, A., and Shanmugam, V. K. (2019). "Anti-inflammatory mechanism of various metal and metal oxide nanoparticles synthesized using plant extracts: A review," *Biomed. Pharmacother.* 109, 2561-2572. DOI: 10.1016/j.biopha.2018.11.116

Ali, Z. (1999). "Acoustic wave mass sensors," *Journal of Thermal Analysis and Calorimetry* 55, 397-412. DOI: 10.1023/A:1010151231380

Babatimehin, A. M., Ajayi, G. O., Ogunbamowo, O. E., El-Rayyes, A., Albedair, L. A., Alsuhaibani, A. M., and Ofudje, E. A. (2025). "Synthesis of silver nanoparticles using *Azadirachta indica* leaf extracts for heavy metal sensing," *BioResources* 20(2), 3342-3366. DOI: 10.15376/biores.20.2.3342-3366

Berna, v. W. d. J., Penaloza-Castañeda, J., Mora, A. M., Corrales-Vargas, A., Eskenazi, B., Hoppin, J. A., and Lindh, C. H. (2024). "Pesticide exposure, birth size, and gestational age in the ISA birth cohort, Costa Rica," *Environmental Epidemiology* 8(2), article e290. DOI: 10.1097/EE9.0000000000000290

Bose, S., Kumar, P. S., and Vo, D. V. N. (2021). "A review on the microbial degradation of chlorpyrifos and its metabolite TCP," *Chemosphere* 283, 131447. DOI: 10.1016/j.chemosphere.2021.131447

Chaudhary, S., Kanwar, R. K., Sehgal, A., Cahill, D. M., Barrow, C. J., Sehgal, R., and Kanwar, J. R. (2017). "Progress on *Azadirachta indica* based biopesticides in replacing synthetic toxic pesticides," *Front. Plant Sci.* 8, article 610. DOI: 10.3389/fpls.2017.00610

Chhangte, V., Samuel, L., Ayushi, B., Manickam, S., Bishwajit, C., and Samuel, L. R. (2021). "Green synthesis of silver nanoparticles using plant extracts and their antimicrobial activities: A review of recent literature," *RSC Adv.* 11, article 2804. DOI: 10.1039/D0RA09941D

Du, J., Jiang, L., Shao, Q., Liu, X., Marks, R. S., Ma, J., and Chen, X. (2012). "Colorimetric detection of mercury ions based on plasmonic *n*anoparticles," *Small* 9(9-10), 1467-1481. DOI: 10.1002/smll.201200811

Foong, S. Y., Ma, N. L., Lam, S. S., Peng, W., Low, F., Lee, B. H., Alstrup, A. K. O., and Sonne, C. (2020). "A recent global review of hazardous chlorpyrifos pesticide in fruit and vegetables: Prevalence, remediation and actions needed," *Journal of Hazardous Materials* 400, article 123006. DOI: 10.1016/j.jhazmat.2020.123006

Fukase, E., and Martin, W. (2020). "Economic growth, convergence, and world food demand and supply," *World Development* 132, article 104954. DOI: 10.1016/j.worlddev.2020.1049

Hassanien, A. S., and Khatoon, U. T. (2018). "Synthesis and characterization of stable silver nanoparticles, Ag-NPs: Discussion on the applications of Ag-NPs as antimicrobial agents," *Physica B: Condensed Matter* 554, 21-30. DOI: 10.1016/j.physb.2018.11.004

Intisar, A., Ramzan, A., Sawaira, T., Kareem, A. T., Hussain, N., Din, M. I., Bilal, M., and Iqbal, H. M. (2022). "Occurrence, toxic effects, and mitigation of pesticides as

emerging environmental pollutants using robust nanomaterials–A review," *Chemosphere* 293, article 133538. DOI: 10.1016/j.chemosphere.2022.133538

Ismail, R. K., Mubarak, T. H., and Al-Haddad, R. M. S. (2019). "Surface plasmon resonance of silver nanoparticles: Synthesis, characterization, and applications," *J. Biochem. Tech*. 10(2), 62-64.

Javid, A., Javed, A. B., and Muhammad, S. (2023). "Comparative bioactive compounds and fourier transform infrared spectroscopic evaluation of *Azadirachta indica* extracts and its potential as bio-fungicides against plant pathogenic fungi," *Intern. J. Eng. Sc. and Technol.* 15(1), 1-12. DOI: 10.4314/ijest.v15i1.1

Jaya, B., Brajesh, B., Gianluca, G., Gabriela, B., and Amit, K. (2022). "Electrochemical sensors and their applications: A review," "*Chemosensors* 10(9), article 363. DOI: 10.3390/chemosensors10090363

Jeevanandam, J., Siaw, F. K., Boakye-Ansah, S., Sie, Y. L., Ahmed, B., Michael, K. D., and João, R. (2022). "Green approaches for the synthesis of metal and metal oxide nanoparticles using microbial and plant extracts," *Nanoscale* 14(7), 2534-2571. DOI: 10.1039/D1NR08144F

Karami-Mohajeri, S., and Abdollahi, M. (2011). "Toxic influence of organophosphate, carbamate, and organochlorine pesticides on cellular metabolism of lipids, proteins, and carbohydrates: A systematic review," *Human and Experimental Toxicology* 30(9), 1119-1140.

Khalil, M. M. H., Ismail, E. H., El-Baghdady, K. Z., and Mohamed, D. (2014). "Green synthesis of silver nanoparticles using olive leaf extract and its antibacterial activity," *Arabian Journal of Chemistry* 7(6), 1131-1139. DOI: 10.1016/j.arabjc.2013.04.007

Khan, A., Vibhute, A. D., Mali, S., and Patil, C. H. (2022). "A systematic review on hyperspectral imaging technology with a machine and deep learning methodology for agricultural applications," *Ecological Informatics* 69, article 101678.

Kushwaha, A., Singh, G., and Sharma, M. (2020). "Colorimetric sensing of chlorpyrifos through negative feedback inhibition of the catalytic activity of silver phosphate oxygenase nanozymes," *RSC Advances* 10(22), 13050-13065. DOI: 10.1039/C9RA10719C

Lee, S.-W., Chang, S.-H., Lai, Y.-S., Lin, C.-C., Tsai, C.-M., Lee, Y.-C., Chen, J.-C., and Huang, C.-L. (2014). "Effect of temperature on the growth of silver nanoparticles using plasmon-mediated method under the irradiation of green LEDs," *Materials* 7, 7781-7798. DOI: 10.3390/ma7127781

Mahmood, W. K., Ibrahim, R. K., and Naje, A N. (2021). "Surface plasmon resonance study of Ag nanoparticles colloidal," *Iraqi Journal of Science* 58(4B), 2090-2097. DOI: 10.24996/ijs.2017.58.4B.12

Matam, P., Dariusz, K., Piotr, K., Dibyendu, M., and Gregory, F. (2021). "Uncovering the phytochemical basis and the mechanism of plant extract-mediated eco-friendly synthesis of silver nanoparticles using ultra-performance liquid chromatography coupled with a photodiode array and high-resolution mass spectrometry," *ACS Sustainable Chem. Eng.* 10(1), 562-571. DOI: 10.1021/acssuschemeng.1c06960

Mercija, J., and Nevaditha, N. T. (2022). "Phytochemical screening and mass spectral analysis of *Azadirachta indica* linn. Gum," *Orient. J. Chem.* 38(2), article 30. DOI: 10.13005/ojc/380230

Mudhafar, M., Zainol, I., Jaafar, C. N., and Alsailawi, H. A. (2020). "Phytochemical screening and quantitative analysis of *Azadirachta indica* leaf extracts," *Journal of Medicinal Plants Research* 14(4), 123-130.

Muthuswamy, S., Krishnamurthy, S., and Yeoung-Sang, Y. (2010). "Immobilization of silver nanoparticles synthesized using *Curcuma longa* tuber powder and extract on cotton cloth for bactericidal activity," *Bioresource Technology* 101, 7958-7965.

Patil, R. B., and Chougale, A. D. (2021). "Analytical methods for the identification and characterization of silver nanoparticles: A brief review," *Materials Today: Proceedings* 47(16), 5520-5532. DOI: 10.1016/j.matpr.2021.03.384

Ritu, K. K. V, Das, A., and Prakash, C. (2023). "Phytochemical-based synthesis of silver nanoparticle: Mechanism and potential applications," *BioNanoSci.* 13, 1359-1380. DOI: 10.1007/s12668-023-01125-x

Roy, P., Das, B., Mohanty, A., and Mohapatra, S. (2017). "Green synthesis of silver nanoparticles using *Azadirachta indica* leaf extract and its antimicrobial study," *Appl Nanosci* 7, 843-850 (2017). DOI: 10.1007/s13204-017-0621-8

Sarkar, S., and Das, R. (2018). "Presence of chlorpyrifos shows blue shift of the absorption peak of silver nanohexagons solution– An indication of etching of nanocrystals and sensing of chlorpyrifos," *Sensors and Actuators B: Chemical*. 266, 149-159. DOI: 10.1016/j.snb.2018.03.123

Shikha, S., Dureja, S., Sapra, R., Babu, J., Haridas, V. and Pattanayek, S. K. (2021). "Interaction of borohydride stabilized silver nanoparticles with sulfur-containing organophosphates," *RSC Adv.* 11, 32286-32294. DOI: 10.1039/D1RA06911J

Sidhu, A. K., Verma, N., and Kaushal, P. (2022). "Role of biogenic capping agents in the synthesis of metallic nanoparticles and evaluation of their therapeutic potential," *Front. Nanotechnol.* 3, article 801620. DOI: 10.3389/fnano.2021.801620

Singh, B. K., and Walker, A. (2006). "Microbial degradation of organophosphorus compounds," *FEMS Microbiology Reviews* 30(3), 428-471.

Taha, A., Ben Aissa, M., and Da'na, E. (2020). "Green synthesis of an activated carbon-supported Ag and ZnO nanocomposite for photocatalytic degradation and its antibacterial activities," *Molecules* 25(7), article 1586. DOI: 10.3390/molecules25071586

Tshilumbu, N. N., Kharatyan, E., and Masalova, I. (2014). "Effect of nanoparticle hydrophobicity on stability of highly concentrated emulsions," *Journal of Dispersion Science and Technology* 35(2), 283-292. DOI: 10.1080/01932691.2013.775584

Uznanski, P., Zakrzewska, J., Favier, F., Kazmierski, S., and Bryszewska, E. (2017). "Synthesis and characterization of silver nanoparticles from (bis)alkylamine silver carboxylate precursors," *J. Nanopart. Res.* 19, article 121. DOI: 10.1007/s11051-017-3827-5

Verma, A., and Mehata, M. S. (2015). "Controllable synthesis of silver nanoparticles using Neem leaves and their antimicrobial activity," *Journal of Radiation Research and Applied Sciences* 9(1), 109-115. DOI: 10.1016/j.jrras.2015.11.001

Villagrán, Z., Anaya-Esparza, L. M., Velázquez-Carriles, C. A., Silva-Jara, J. M., Ruvalcaba-Gómez, J. M., Aurora-Vigo, E. F., Rodríguez-Lafitte, E., Rodríguez-Barajas, N., Balderas-León, I., and Martínez-Esquivias, F. (2024). "Plant-based extracts as reducing, capping, and stabilizing agents for the green synthesis of inorganic nanoparticles," *Resources* 13, article 70. DOI: 10.3390/resources13060070

Ying, S., Guan, Z., Ofoegbu, P.C., Clubb, P., Rico, C., He, F., and Hong, J. (2022). "Green synthesis of nanoparticles: Current developments and limitations," *Environ. Technol. Innov.* 26, article 102336. DOI: 10.1016/j.eti.2022.102336

Zhang, Y., Jia, Q., Hu, C., Han, M., Guo, Q., Li, S., Bo, C., Zhang, Y., Qi, X., Sai, L. and Peng, C. (2021). "Effects of chlorpyrifos exposure on liver inflammation and intestinal flora structure in mice," *Toxicology Research* 10(1), 141-149. DOI: 10.1093/toxres/tfaa108

Zhang, X., Li, W., Li, W., Yue, L., Zhang, T., Tang, Q., Zhang, N., Lan, X., and Pan, C. (2023). "Chlorpyrifos induces male infertility in pigs through ROS and PI3K-AKT pathway," *iScience* 26(5), article 106558. DOI: 10.1016/j.isci.2023.106558

Article submitted: March 25, 2025; Peer review completed: April 26, 2025; Revised version received: May 7, 2025; Accepted: June 11, 2025; Published: June 27, 2025.
DOI: 10.15376/biores.20.3.6948-6965